Impact of the LCD monitor locations on a novel alignment method: the combination of deflectometry and the sine condition test

Hyemin Yoo, Matthew Dubin

Hyemin Yoo, Matthew Dubin, "Impact of the LCD monitor locations on a novel alignment method: the combination of deflectometry and the sine condition test," Proc. SPIE 12222, Optical System Alignment, Tolerancing, and Verification XIV, 1222206 (3 October 2022); doi: 10.1117/12.2639735

SPIE.

Event: SPIE Optical Engineering + Applications, 2022, San Diego, California, United States

Impact of the LCD monitor locations on a novel alignment method: the combination of deflectometry and the sine condition test

Hyemin Yoo and Matthew Dubin*
Wyant College of Optical Sciences, the University of Arizona, 1630 E. University Blvd, Tucson, AZ, USA 85721

ABSTRACT

We have proposed a new alignment method which is the combination of deflectometry and the sine condition test. One of the great advantages of the new approach is that we need a camera and an LCD monitor larger than the clear aperture of the telescope instead of an interferometer and a return flat. To determine the state of the alignment, we have to place the monitor at two different locations: ideally at the rear principal plane of the telescope and a few meters displaced from the rear principal plane. However, for practical reasons, we may have to place the monitor closer to the telescope. We have simulated how changing the monitor location impacts the alignment, and we show the consequences of variations in the LCD locations on the alignment of a telescope using the new method.

Keywords: Alignment, deflectometry, sine condition test

1. INTRODUCTION

Alignment is an essential step for manufacturing a telescope successfully [1]. Even the simplest form of telescope requires an alignment process for properly positioning its optical elements to avoid aberrations. To achieve an accurate alignment, it is necessary to aim for accurate measurements of the low order misalignment aberrations: linearly-field dependent astigmatism (linear astigmatism), linearly-field dependent focus (linear focus), power, spherical and constant coma. A conventional way of aligning a two-mirror telescope is an interferometric alignment with a return flat placed in the collimated space of the telescope and an interferometer at the finite conjugate point [2]. This is a very powerful method, but it can be an issue when people want to build a meter-class telescope because it requires an expensive, meter-sized return flat for alignment.

Yoo and Dubin [3] developed a new alignment method that is an economical choice for engineers looking for an alternative alignment plan for a meter-class telescope project. The combination of deflectometry and the sine condition test is a novel approach for alignment which is a simple on-axis setup composed of a pixelated camera and a monitor. For a meter-class telescope, an 82-inch LCD TV can be purchased with a market price of under two thousand dollars. The deflectometry part of the new alignment method measures power, spherical, and constant coma, while the sine condition test part measures linear astigmatism and linear focus. It can provide complete information on the aberrations indicating misalignment, and, at the same time, it can measure all of them with on-axis measurements, which makes it easier for a mounting plan as moving testing tools to multiple field points are unnecessary. Instead, we simply need to slide the LCD TV to at least two positions in the collimated space, and, more importantly, absolute positioning is not required for the LCD.

In this paper, we would like to provide more information about the practical implementation of the new alignment method. As Yoo and Dubin [3] focused on explaining the concept, it is necessary to show several details related to the LCD monitor positions which can improve the performance of the new alignment approach. We will explain the concept briefly, but we want to focus on presenting several simulation results which show the impact of the monitor positions on the alignment result.

*mdubin@optics.arizona.edu; phone 1 520 626-3723; fax 1 520 626-3723; https://wp.optics.arizona.edu/oeff/

Optical System Alignment, Tolerancing, and Verification XIV, edited by José Sasián, Richard N. Youngworth, Proc. of SPIE Vol. 12222, 1222206 · © 2022
SPIE · 0277-786X · doi: 10.1117/12.2639735

2. THE NEW ALIGNMENT METHOD

2.1 Deflectometry

The deflectometry part of the new alignment method measures misalignment aberrations that are on-axis aberrations: power, spherical, and constant coma. This can be done by placing the monitor in at least two on-axis positions. Figure 1 shows the on-axis setup applied to a Ritchey-Chrétien telescope. The telescope is located between the camera and the monitor. In reality, light starts from a monitor pixel, as the LCD monitor is the source. For convenience, however, we assume that a ray starts from a detector pixel, goes through the center of the camera pupil, and reaches a corresponding monitor pixel. Software is used to determine where on the monitor this ray lands with sub-pixel accuracy.

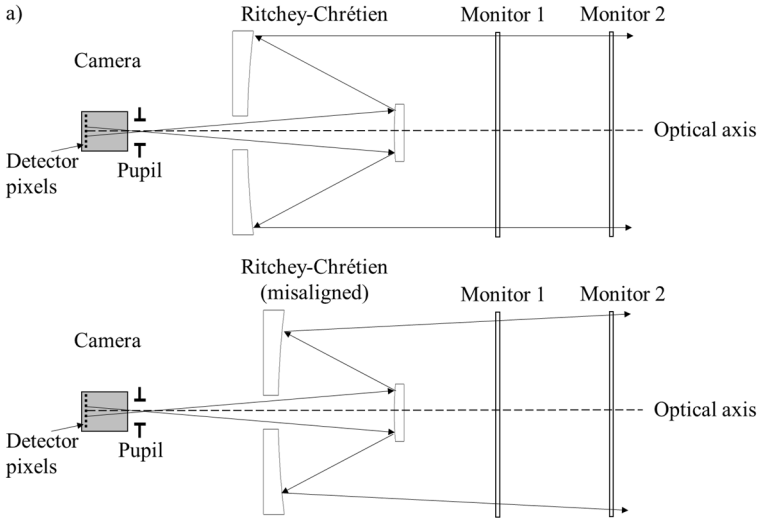

Figure 1. The concept of deflectometry in the new alignment method applied to a Ritchey-Chrétien telescope. (a) is the case without any on-axis aberration. Two rays defined by detector pixels propagate into the telescope and are parallel to the optical axis in collimated space. (b) is when the distance between two mirrors in the telescope is shifted from the nominal design. The same rays from (a) are diverging in this case.

Comparing the two illustrations in Figure 1 explains how the relative measurement of a change in ray locations at the monitor planes can be useful. In Figure 1(a), the center of the camera pupil is placed at the focal point of the telescope and the monitor planes are placed perpendicular to the optical axis in the infinite conjugate space. This configuration simulates a system where there is no wavefront error caused by on-axis aberrations. Therefore, the spacings between the rays at the first and second monitor planes are the same. Figure 1(b) shows what happens when the spacing between the two mirrors is different from the nominal design. It means there are on-axis aberrations, spherical and power, in the system. The key point is that the spacing between the rays at the two monitor planes changes. These relative changes in ray position between the two monitor planes are what we want to measure. We can calculate the amount of on-axis aberration in the system with these measurements. The collection of relative differences in the ray intersections is named the slope mapping error.

2.2 Sine condition test

The remaining aberrations, linear astigmatism and linear focus, can be measured with the sine condition test part of the new method. The goal of this step is to measure if the system satisfies the sine condition. It measures errors such as Seidel coma, linear astigmatism, and linear focus. Seidel coma is an indicator of sine condition violation when the system is axially symmetric, while the other two are generated from plane-symmetric errors [4]. The sine condition for a finite/infinite conjugate system is

$$h = f_{eff} sin(\theta), \tag{1}$$

Where h is the height of a ray in infinite conjugate space, f_{eff} is the effective focal length of the system, and θ is the angle of the ray in finite conjugate space [5]. If a system under test violates this condition, it does not satisfy the sine condition, and, therefore, it will have linearly field dependent aberrations.

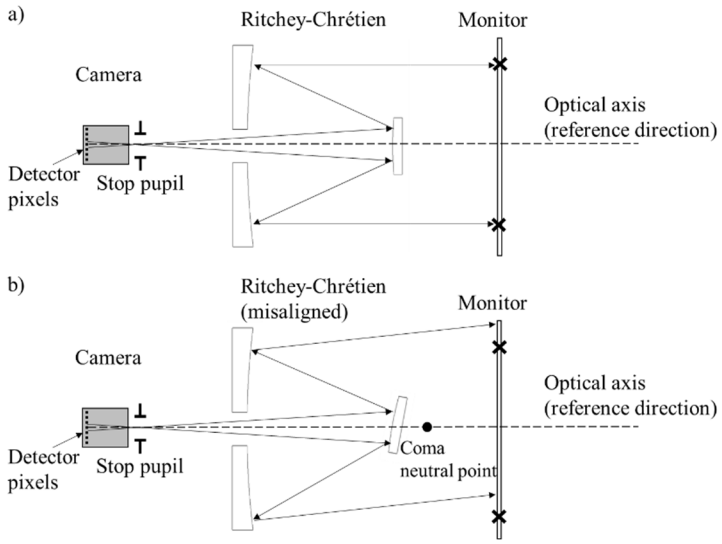

Figure 2. The concept of the sine condition test in the new alignment method applied to a Ritchey-Chrétien telescope. (a) Ritchey-Chrétien telescopes are spherical and Seidel coma-free. Therefore, there is no difference between the ideal intersections (cross marks) and the real ray intersections. (b) is when the secondary is pivoted about the coma-neutral point causing linear astigmatism, which means the system violates the sine condition. The rays are parallel to each other, but they are not parallel to the optical axis. As a result, the ideal intersections and the real ray intersections are different.

Figure 2 shows the Ritchey-Chrétien telescope as an example. The cross marks show ideal ray intersections, which can be calculated with Equation (1) by assuming that the system satisfies the sine condition. Figure 2(a) is an illustration of the perfect design, with no misalignment. As the Ritchey-Chrétien is an aplanatic system, there is no Seidel coma. Therefore, there is no difference between the real ray intersections and the ideal intersections. Figure 2(b) shows when the secondary is pivoted about the coma-neutral point of the telescope. This action breaks the axial symmetry of the system and causes linear astigmatism which indicates the sine condition violation. The measurement of the height difference between the real ray intersections and the ideal ray intersections contains information on how much linear astigmatism is present in the system. Other misalignments that break the axial symmetry can also produce linearly-field dependent aberrations. For the alignment, we measure the collection of differences in the ray intersections, which is called the pupil mapping error.

2.3 Mapping errors

The principle of the new alignment method is measuring the mapping errors, pupil mapping error and slope mapping error, from the monitor planes. The mapping errors are two-dimensional vector fields, so to analyze the mapping errors, we use S and T polynomials proposed by Zhao and Burge [6, 7]. These polynomials are a vector basis set derived from gradients of Zernike polynomials. We select S and T terms that are orthogonal to each other and also represent the mapping errors that correspond to the aberrations of misalignment. For the pupil mapping error, S7, S8, T7, and T8 are required to describe linear astigmatism and linear focus. For the slope mapping error, we add Δ before terms to indicate that these are relative differences between mapping errors measured from two monitor planes. We need ΔS4, ΔS7, ΔS8, and ΔS11 to describe power, constant coma, and spherical. Details of the forms of the vector fields and their related terms and ratios for each alignment aberration can be found in Yoo and Dubin [3].

It gets clearer why we need to measure mapping errors from more than one position when we look at the features of the mapping errors. Figure 3(a) is an example of a mapping error that is rotationally symmetric and radially cubic dependent. When this feature is observed from the pupil mapping error, this means there is a Seidel coma in the system. If it is seen from the slope mapping error, there is spherical aberration.

Theoretically, the rear principal plane is recommended as the first monitor location. This is because according to the first order optics, the on-axis wavefront error will not contribute to the mapping error at that location. Therefore, the mapping error we get from the rear principal plane is solely a pupil mapping error. Then, we can move the monitor a meter further from the first position, and the difference between the first and second positions is a slope mapping error.

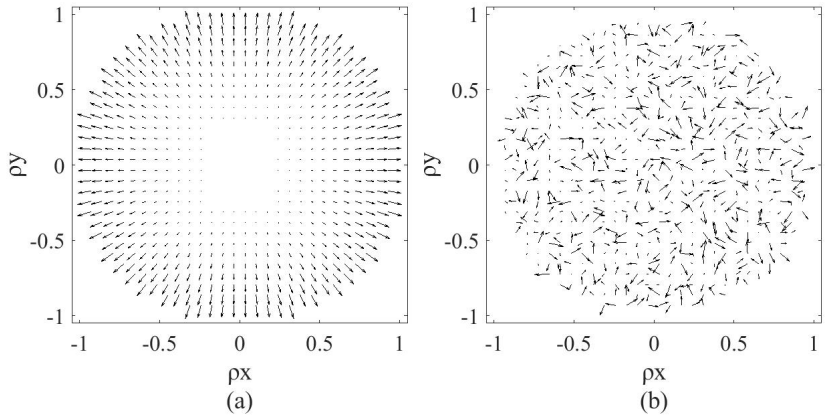

Figure 3. Mapping error examples. (a) has a cubic dependence along the radius and is rotationally symmetric. (b) is an example of a mapping error caused by pixel noise.

However, this may be an impractical choice for an alignment plan in reality. If the rear principal plane is a few tens of meters away from the secondary mirror, we could face difficulties that make the alignment plan even more complicated. Therefore, this is necessary to check if moving the monitors much closer to the telescope, like a distance comparable to the telescope length, would impact the final alignment. Also, among various sources of noise, uncertainty in the monitor pixels, *pixel noise*, is a driving factor of the new method. According to Su et al. [8], there is 1/10-pixel uncertainty which is random noise in the measurement of pixel positions. This can be interpreted as Figure 3(b), which is a collection of vectors in random directions and sizes between 0 to 1/10 of a pixel. This mapping error "error", which we prefer to label as *δME*, contains the eight S and T terms we care about that are comparable to magnitudes of those terms from pupil and slope mapping error. This can be thought of as a signal-to-noise ratio problem where mapping errors are the signal, and δME from pixel noise is the noise. If we can increase the signal-to-noise ratio, this means that we can improve the final alignment. In the following section, we will discuss the simulation studies we did to provide information on practical choices for the implementation of the new alignment for real telescope projects.

3. IMPACT OF THE LCD MONITOR POSITIONS

3.1 Simulation preparations

To show the impact of the LCD monitor positions on the new alignment method, we present the results from our simulation. A simple Ritchey-Chrétien telescope was designed as a unit-under-test. This telescope is F/9.3 with a 1 m clear aperture. The primary is F/0.9. We assume that M1 is fixed in location and the other elements are aligned to it. Also, the location of the camera pupil defines the location for the telescope sensor. The center of the pupil is the location for the center of the sensor, and the direction of the ray coming from the center of the camera through the center of the pupil defines the surface normal of the sensor.

Table 1. Ten perturbations (DOFs) applied to the telescope

DOF number	DOF descriptions	Tolerance range	Units
1	Pupil to M2 distance	±0.5	mm
2	Pupil decenter in x	±0.5	mm
3	Pupil decenter in y	±0.5	mm
4	M2 to M1 distance	±0.5	mm
5	M2 decenter in x	±0.5	mm
6	M2 decenter in y	±0.5	mm
7	Pupil tilt about x	±5.0	mrad
8	Pupil tilt about y	±5.0	mrad
9	M2 tilt about x	±5.0	mrad
10	M2 tilt about y	±5.0	mrad

There are ten possible perturbations in the test setup for the Ritchey-Chrétien. Table 1 summarizes the list of perturbations used in the simulation as well as their tolerance range.

After a perturbed telescope was created, a ray-tracing macro was applied to get real ray intersections at monitor planes. The ideal ray intersections can be calculated because a detector pixel defines a ray. By setting a reference direction that is determined by the center of the detector plane and the center of the camera stop, we can also define a ray angle, θ, using the coordinate of the detector pixel, (x_{det}, y_{det}), and the effective focal length of the camera, f_{camera}.

$$\theta = tan^{-1}\left(\frac{\sqrt{{x_{det}}^2+{y_{det}}^2}}{f_{camera}}\right), \quad (2)$$

Then, the ideal height of the ray based on the sine condition can be calculated using Equation (1). We can derive mapping errors by taking the differences between the ideal ray locations on the monitor and the real ray locations. Measured pupil and slope mapping errors are analyzed using the sensitivity matrix of the telescope, and we calculate the changes necessary to align the perturbed telescope. We did three iterations of alignment for each trial. The simulation also contains the sources of noise, not only the pixel noise, but also others such as mirror fabrication errors, uncertainty in camera distortion correction, LCD monitor sag, and its positional error. Table 2 summarizes how the sources of noise were applied to the simulation.

Table 2. The sources of noise description

Type	Descriptions	Tolerance range
Pixel noise	1/10 of a monitor pixel size	0.00-0.05 mm (magnitude), ±π (direction)
Distortion error	Maximum distortion	±0.1%
Fabrication error	RMS Zernike surface sag	±50 nm (Z4-Z11), ±5 nm (Z12-Z37)
LCD sag error	FEA modeling of LCD monitor sag	
LCD positioning	Decenters, spacing, and tilts of the monitor planes	±0.5 mm or ±5.0 mrad

To describe the performance of the alignment, we use a new metric proposed by Yoo and Dubin [3]. Unlike conventional ways, such as residual wavefront error, we do not want to include errors in the telescope system that cannot be aligned out. Sag errors like trefoil on both mirrors are a good example. Fuerschbach et al. [9] indicated that the combination of trefoil causes a different form of linear astigmatism, which is called field linear, field conjugate astigmatism. This is also linear astigmatism, but different from linear astigmatism caused by misalignments. The important point is that it cannot be removed by adjusting the positions of the optics. We have defined a term, *the Metric for Misalignment Indicators (MMI)* that only includes the errors due to the aberrations of misalignment. MMI may not be a direct measurement of the maximum change in the wavefront, but it is a measurement of the maximum wavefront error possible due to the alignment errors in the system.

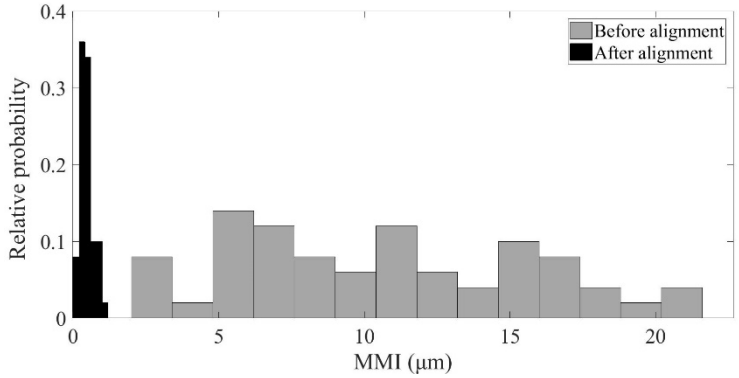

Figure 4. Normalized histogram of the MMI before and after alignment. The area under each histogram is one.

We created 50 configurations of the perturbations where each error was randomly generated within uniform probability distribution. Using the same configuration, we tried several cases of monitor positions. To do this, we created a sensitivity matrix for each case, and we used it for alignment. We used simulations with the first monitor at the rear principal plane

and the second monitor at a 1 m distance from the first monitor as the nominal case. As the distance between two monitor planes is 1 m, the difference between the mapping errors from the two positions, *ΔME,* should be the slope mapping error for the system. Figure 4 shows the state of alignment before and after 3 iterations. Before alignment, the average MMI was 10.56 μm with a standard deviation of 5.04 μm. The aligned systems have an average MMI of 0.47 μm with a standard deviation of 0.22 μm.

3.2 First and second monitor planes separation

While the results for the nominal monitor locations produced a significant improvement in the state of alignment, it is reasonable to think that increasing the separation between the monitor positions should make things even better. This is straightforward if we think of it as a signal-to-noise ratio problem. Slope mapping error (SME) is calculated by the ratio of the difference between mapping errors from the two monitor planes, ΔME, and the separation of the two planes, *s*, which yields

$$SME = \frac{\Delta ME}{s}. \tag{3}$$

However, with the presence of noise, measured ΔME, *ΔME(measured)*, is not purely from the slope errors caused by misalignments. If we call pure slope error as *ΔME(pure)*, then we can rewrite Equation (3) as,

$$SME = \frac{\Delta ME(measured)}{s} = \frac{\Delta ME(pure) + \delta ME}{s} = SME(pure) + \frac{\delta ME}{s}. \tag{4}$$

We can consider SME(pure) and δME/s, analogous to signal and noise. Then, the signal-to-noise ratio can be written as

$$SNR = \frac{SME(pure)}{(\delta ME/s)}. \tag{5}$$

According to Equation (4) and Equation (5), we can see that if the separation, s, gets bigger, then the SNR increases which means a better estimation of the SME.

To demonstrate this, we performed two different sets of simulations; the only difference between the first and the second set is the separation between two monitor planes: 1 m separation vs. 5 m separation. For both sets, the first monitor plane is at the rear principal plane. It is clear that when the separation is longer, the alignment results get better. The 1 m separation, after alignment, has an average of MMI 0.47 μm with a standard deviation of 0.22 μm. The 5 m separation has an average of MMI 0.11 μm with a standard deviation of 0.04 μm. As expected, the improvements are found in the on-axis aberrations. The standard deviation of power is improved by 0.08 μm, constant coma by 0.04 μm. The off-axis aberrations were also improved. Linear focus by 0.15 μm, and linear astigmatism by 0.1 μm.

3.3 Telescope and first monitor plane separation

As mentioned earlier, using the rear principal plane is a theoretical recommendation that may not be realistic. For example, the rear principal plane of the Ritchey-Chrétien telescope model in this simulation is 47.4 meters away from the primary mirror. Therefore, we wanted to see if the performance of the new alignment method would degrade when we bring the monitor planes closer to the telescope. For this simulation, we set the first monitor at 1 m away from the primary, which is 0.23 m away from the secondary. The second monitor plane is placed 1 m further away from the first monitor plane. After bringing the monitor planes closer to the telescope, the average of MMI is 0.16 μm with a standard deviation of 0.05 μm. When we look at the aberrations individually, we observe the standard deviations of linear astigmatism and linear focus improved by 0.11 μm and 0.17 μm each. There is not much difference in the on-axis aberrations.

Our expectation was that we would get similar performance with the monitors closer. The SNR for slope mapping error should be the same, and when the mapping error for the two monitor positions is the same, the sine condition is satisfied regardless of where the monitors are located. In other words, measuring away from the principal plane should still work. The sensitivity matrix, however, shows there is a difference in the sensitives to M2 tilts and decenters, and this is consistent with the improvements we saw.

Based on these results, it was logical to try a 5 m separation with the first monitor position closer to the telescope. When we did this, we got the best performance with an average MMI of 0.08 μm and a standard deviation of 0.03 μm. The improvement is dramatic when the first monitor plane is closer to the telescope and the separation between the first and

second monitor planes is larger. Table 3 summarizes the average values and standard deviations of the MMI for the four simulations showing how the monitor positions improve the alignment.

Table 3. Summary of the simulations (Impact of the monitor positions)

	Average (μm)		Standard deviation (μm)	
	Separation 1 m	Separation 5 m	Separation 1 m	Separation 5 m
First monitor at RP	0.47	0.11	0.22	0.04
First monitor Closer	0.16	0.08	0.05	0.03

4. CONCLUSIONS

The purpose of this paper is to explain how the monitor positions can help improve the performance of the new alignment method utilizing deflectometry and the sine condition. When the first monitor plane is close to the telescope and the separation between the two monitor planes is larger, the residual errors in the system decrease significantly from our nominal case. This shows that not only can a telescope be accurately aligned with a camera and LCD monitor, the selection of where the monitor is placed can have a significant impact on the quality of the alignment.

REFERENCES

[1] Roland V. Shack and Kevin Thompson, “Influence of alignment errors of a telescope system on its aberration field”, Proc. SPIE 0251, 146-153 (1980).

[2] Eric P. Goodwin and James C. Wyant, [Field Guide to Interferometric Optical Testing], SPIE Press, Bellingham, 53-54 (2006).

[3] Yoo and Dubin, “Alignment with a combination of deflectometry and the sine condition test”, (in prep).

[4] J. H. Burge, C. Zhao, and M. Dubin, “Use of the Abbe sine condition to quantify alignment aberrations in optical imaging systems,” Proc. SPIE **7652**, International Optical Design Conference 2010, 765219 (2010).

[5] J. H. Burge, C. Zhao, M. Dubin, and S. Lampen, "Determination of off-axis aberrations of imaging systems using on-axis measurements," Proc. SPIE **8129**, 81290F (2011).

[6] C. Zhao and J. H. Burge, "Orthonormal vector polynomials in a unit circle, Part I: basis set derived from gradients of Zernike polynomials, " Opt. Express **15**, 18014-18024 (2007).

[7] C. Zhao and J. H. Burge, "Orthonormal vector polynomials in a unit circle, Part II: completing the basis set, " Opt. Express 16, 6586-6591 (2008).

[8] P. Su, R. E. Parks, L. Wang, R. P. Angel, and J. H. Burge, "Software configurable optical test system: a computerized reverse Hartmann test," Appl. Opt. **49**, 4404–4412 (2010).

[9] K. Fuerschbach, J. P. Rolland, and K. P. Thompson, "Extending nodal aberration theory to include mount-induced aberrations with application to freeform surfaces, " Opt. Express **20**, 20139–20155 (2012).